iScience

CellPress
OPEN ACCESS

Article

Innate immune sensing of influenza A viral RNA through IFI16 promotes pyroptotic cell death

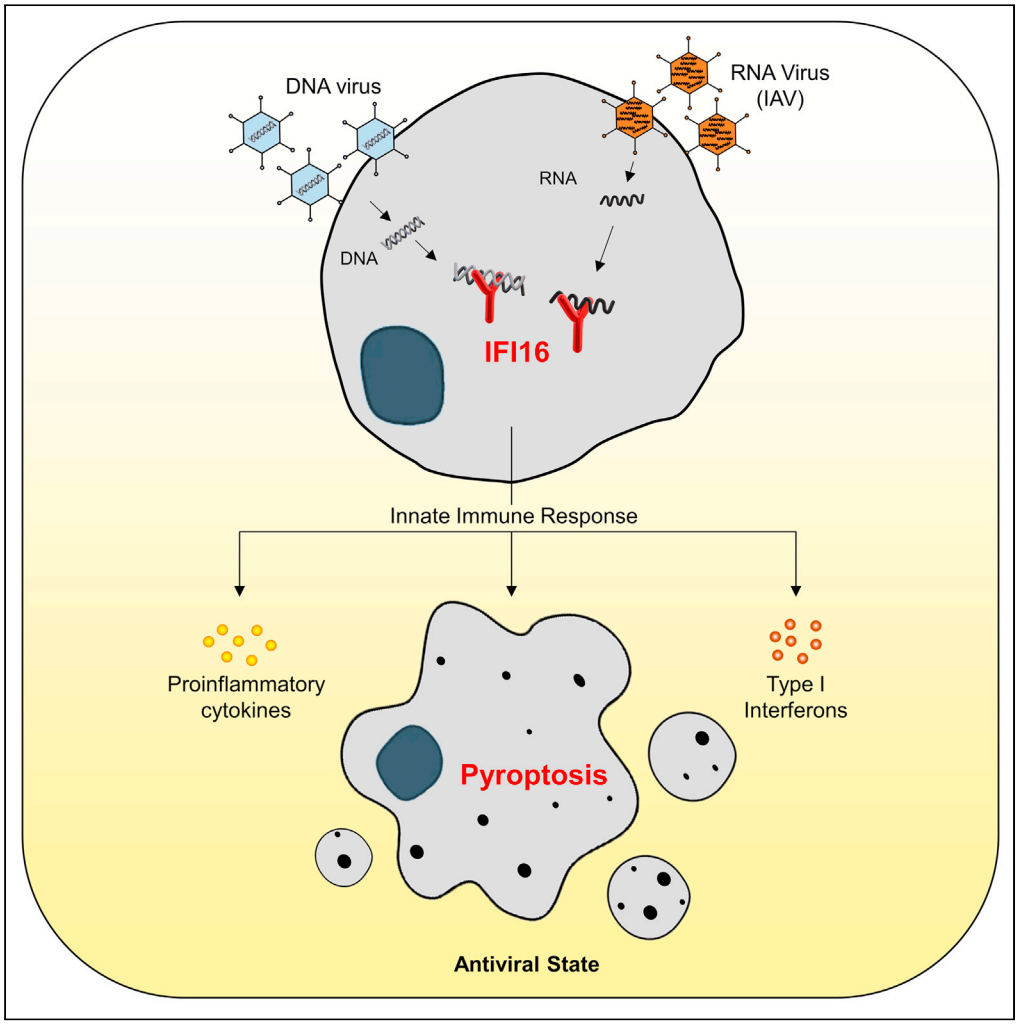

Shalabh Mishra, Athira S. Raj, Akhilesh Kumar, Ashwathi Rajeevan, Puja Kumari, Himanshu Kumar

hkumar@iiserb.ac.in

Highlights

DNA sensor IFI16 senses Influenza viral RNA

IFI16 induce pyroptosis in Influenza A Virus (IAV) infected cells

IFI16 interacts with IAV RNA and restricts viral replication

IFI16 promotes overall antiviral state during IAV infection

Mishra et al., iScience 25, 103714
January 21, 2022
https://doi.org/10.1016/j.isci.2021.103714

iScience

CellPress
OPEN ACCESS

Article

Innate immune sensing of influenza A viral RNA through IFI16 promotes pyroptotic cell death

Shalabh Mishra,[1,3] Athira S. Raj,[1,3] Akhilesh Kumar,[1] Ashwathi Rajeevan,[1] Puja Kumari,[1] and Himanshu Kumar[1,2,4,*]

SUMMARY

Programmed cell death pathways are triggered by various stresses or stimuli, including viral infections. The mechanism underlying the regulation of these pathways upon Influenza A virus (IAV) infection is not well characterized. We report that a cytosolic DNA sensor IFI16 is essential for the activation of programmed cell death pathways in IAV infected cells. We have identified that IFI16 functions as an RNA sensor for the influenza A virus by interacting with genomic RNA. The activation of IFI16 triggers the production of type I, III interferons, and also pro-inflammatory cytokines via the STING-TBK1 and Pro-caspase-1 signaling axis, thereby promoting cell death (apoptosis and pyroptosis in IAV infected cells). On the contrary, IFI16 knockdown cells showed reduced inflammatory responses and also prevented cell mortality during IAV infection. Collectively, these results demonstrate the pivotal role of IFI16-mediated IAV sensing and its essential role in activating programmed cell death pathways.

INTRODUCTION

The past century has witnessed several pandemics disrupting the socioeconomic harmony of humankind. The influenza pandemic of 1917 and the current novel coronavirus pandemic are examples of the devastation caused by newly evolved viruses. The short replication time of viruses helps them acquire zoonotic potential through numerous mutations over a short period. Influenza is a substantial threat to public health as it causes multiple catastrophic pandemics, killing millions of people around the world. It has a segmented genome and a relatively high mutation rate, leading to better survivability (Carrasco-Hernandez et al., 2017) and evolvability (Duffy, 2018). This eight segmented negative-sense single-stranded RNA virus from the Orthomyxoviridae family naturally infects diverse species, including birds and mammals. Mixing up or exchanging various genomic segments (antigenic shift) during coinfection in an intermediate host can result in the emergence of new viral strains (Webster et al., 1982). Apart from the pandemics, seasonal Influenza virus infections account for more than 5 million cases annually, severely affecting children and older adults (Iuliano et al., 2018; Thompson et al., 2003). An effective therapeutic strategy against emerging influenza virus strains is perplexing because it mutates very fast and subverts host immunity and cellular machinery. However, advanced therapeutic approaches targeting host factors, essential for establishing viral infection, can prove to be more effective.

The RNA genome of Influenza A virus (IAV) in infected cells is sensed by evolutionarily preserved germline-encoded pathogen recognition receptors (PRRs), including Toll-like Receptors (TLR) 3 and 7 (Le Goffic et al., 2007), Retinoic acid-inducible gene I (RIG-I) (Liu et al., 2015), NOD-like receptor family member NOD-, Leucine-rich repeat (LRR)- and pyrin domain-containing 3 (NLRP3) (Thomas et al., 2009), and the Z-DNA binding protein 1 (ZBP1) (Kuriakose et al., 2016; Thapa et al., 2016) in distinct cellular compartments. Upon sensing, the PRRs elicit an array of signaling pathways leading to the innate antiviral state through robust production of type I, III interferons, and pro-inflammatory cytokines via different transcription factors like nuclear factor kappa-light-chain-enhancer of activated B cells (NF-κB) and interferon regulatory factors (IRFs). Interferons further sensitize neighboring cells by inducing Interferon Stimulated Genes (ISGs) and collectively develop a potent antiviral state. In addition to this complex innate immune signaling cascade, interferons and pro-inflammatory cytokines also induce programmed cell death in virus-infected cells.

Programmed cell death is classified into various types based on the cues leading to cell death and macroscopic morphological variations. It has been observed in vitro and in vivo that the IAV induces apoptosis

[1]Department of Biological Sciences, Laboratory of Immunology and Infectious Disease Biology, Indian Institute of Science Education and Research (IISER) Bhopal, Bhopal 462066, MP, India

[2]WPI Immunology, Frontier Research Centre, Osaka University, Osaka 5650871, Japan

[3]These authors contributed equally

[4]Lead contact

*Correspondence: hkumar@iiserb.ac.in

https://doi.org/10.1016/j.isci.2021.103714

(Chen et al., 2001), primary necrosis (Mosavi et al., 2015), necroptosis (Sanders et al., 2013), and pyroptosis (Lee et al., 2018; Stasakova et al., 2005) in various cell types. Virus-associated programmed cell death was initially perceived as a host defense mechanism that limits viral replication by eliminating infected cells. However, recent studies indicate that IAV can manipulate host immunity to induce cell death, helping its propagation. The IAV proteins NS1 (Chung et al., 2015; Moriyama et al., 2016; Stasakova et al., 2005), M1 (Halder et al., 2011), PB1-F2 (Chen et al., 2001; Zamarin et al., 2005), and NP (Tripathi et al., 2013) have been reported to activate apoptotic pathways to evade inflammatory responses and defend their replicative niche. The types of cell death pathways elicited upon IAV infection are mostly known. However, the innate immune sensing and signaling pathways deciding the fate of the cell upon IAV infection remain poorly understood.

This study reports the previously unknown role of well-known PRR Interferon Gamma Inducible protein (IFI) 16 in eliciting cell death in alveolar epithelial cells during IAV infection. IFI16 is an intracellular DNA sensor mediating TBK-1-dependent IFNβ production via an adaptor STING. One of the AIM2-like Receptor (ALR) family members, IFI16, contains an N-terminal Pyrin domain (PYD) and two C-terminal HIN domains that bind to DNA in a sequence-independent manner (Unterholzner et al., 2010). IFI16 was thought to be a cytosolic sensor, but recent studies show that it contains a multipartite nuclear localization signal (NLS) and senses nucleic acid in cytoplasm and nucleus in a PAMP-localization-dependent manner (Li et al., 2012). IFI16 plays a critical role during various DNA viruses (KSHV (Kerur et al., 2011; Singh et al., 2013), HSV-1 (Unterholzner et al., 2010), EBV (Jakobsen et al., 2013), HCMV (Li et al., 2013)), retrovirus (HIV (Jakobsen et al., 2013)), and bacterial infections (*Listeria Monocytogenes* (Hansen et al., 2014)) by restricting pathogens' propagation. Several DNA virus proteins have evolved to inhibit or degrade IFI16, highlighting its vital role in defense against infections (Orzalli et al., 2012; Zhai et al., 2013). Recent studies show that IFI16 can also restrict various RNA virus infections (Sendai (Thompson et al., 2014), EMCV (Thompson et al., 2014), and CHIKV (Wichit et al., 2019)). However, the mechanism by which IFI16 defends against RNA viruses remains elusive, especially IAV infection. Through high-throughput transcriptomic analysis after IFI16 knockdown, we uncovered the mechanistic insights about how IFI16 protects the host against the IAV. Our study shows that IFI16 restricts the IAV infection by interacting with viral RNA (predominantly in the nucleus) and stimulating cell death.

RESULTS

IAV induces cell death in IFI16 dependent manner

To decipher the role of RNA virus-sensing pathways in IAV induced cell death, we performed shRNA mediated transient knockdown of TLR adaptor MyD88 and the RLR adaptor IPS-1, and the adaptor for DNA-sensing pathway STING in human alveolar epithelial (A549) cells followed by Influenza A Virus (IAV) A/Puerto Rico/8/34 (PR8/H1N1) infection (Figure S1A). Cells with STING knockdown showed the most resistance to IAV-induced cell death (Figure S1B). In addition, it has been previously reported that cells lacking the IFN-receptor were fully resistant to IAV-induced cell death (Kesavardhana et al., 2017). This suggests that IFN-mediated signaling plays an essential role in cell death upon IAV infection. To identify IFN-signaling genes that may have a possible role in IAV-mediated cell death, we reanalyzed the publicly available transcriptomic data from the NCBI-GEO database obtained from A549. Comparative analysis of uninfected and IAV-infected cells revealed a significant increase in the expression of nucleic-acid sensors and pro-inflammatory cytokines.

Interestingly, one of the most consistently upregulated nucleic-acid sensors in IAV-infected samples was the gene IFI16 (Interferon Gamma Inducible Protein 16) (Figure S1C). IFI16 has previously been identified as a cytosolic-double-stranded (ds) DNA sensor, which initiates type-I interferon dependent responses. Thus, IFI16 was of potential interest because its role in regulating the Influenza virus is not known, an RNA virus, and inducing cell death.

To probe the role of IFI16 in IAV induced cell death, IFI16 was knocked down in A549 cells using gene-specific shRNA (Figure S2A), and cell death in IAV-infected cells was analyzed by MTT assay, Trypan-blue exclusion, propidium iodide (PI), and also by Annexin-PI FACS. We found that IFI16 knockdown cells were more than 80% resistant to IAV-induced cell death (Figures 1A–1D and S2B). Notably, IFI16 knockdown cells were resistant to cell death induced by IAV but not by another RNA virus, Newcastle Disease virus (NDV), suggesting an IAV-specific, IFI16-dependent cell death. Taken together, these data suggest a critical role of IFI16 in the regulation of cell death/survival during IAV infection.

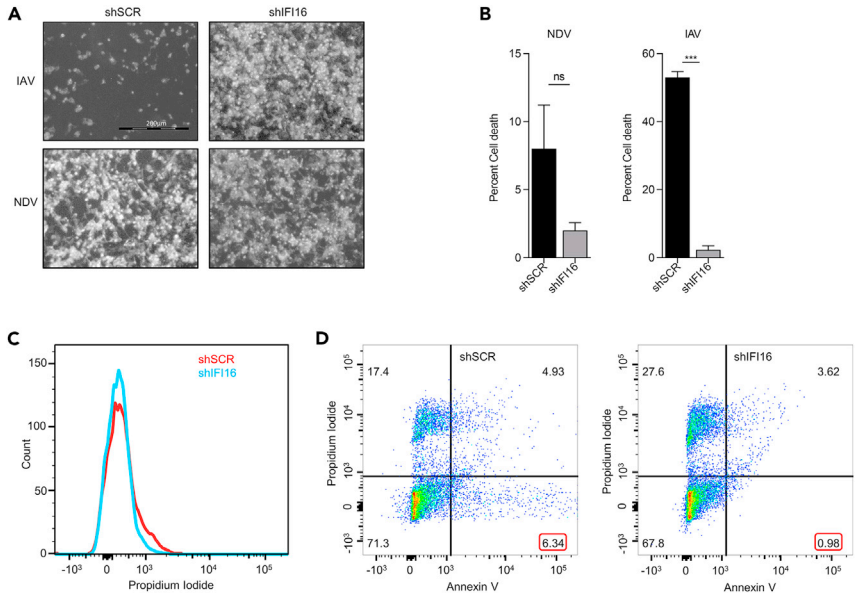

Figure 1. IAV induces cell death in IFI16 dependent manner

(A and B) A549 cells were transiently transfected with 2.0 μg either shRNA of IFI16 (shIFI16) or nonspecific scrambled control (shSCR) for 48 h then infected with IAV (MOI 10) (Upper panel) and NDV (MOI 2) (lower panel). 24 h post images were taken using a 10× objective lens on an inverted microscope, and the cell viability was determined using the MTT assay.

(C and D) 24 h post IAV infection, cells were stained with Propidium Iodide (PI) alone and PI + annexin V/, and apoptosis was determined by using flow cytometric analysis. Data are mean ± SEMs from triplicate samples of a single experiment and are representative of results from three independent experiments. ****, $p < 0.0001$, ***, $p < 0.001$, **, $p < 0.01$, and *, $p < 0.05$, by two-tailed unpaired t test (B). ns, nonsignificant.

IFI16 regulates apoptotic genes in IAV infected cells

To gain mechanistic insights into IFI16-mediate cell death, we performed whole transcriptome analysis of A549 cells transfected either with shSCR or shIFI16, followed by infection with IAV for 24 h, and subjected to RNA-Seq analysis in duplicates as shown in the schematic (Figure 2A). Principal component analysis of the gene expression demonstrates that samples cluster in distinct groups according to their treatment (Figure 2B). Differential gene expression analysis revealed that 947 genes were significantly upregulated, whereas 822 genes were downregulated (Figure 2C). Moreover, pathway analysis of significantly dysregulated genes using different tools indicated that IFI16 knockdown leads to the downregulation of interferon signaling pathways, TNF and NF-κB signaling, and caspase-mediated apoptosis signaling pathways (Figure 2D). We noticed that a large number of genes associated with the apoptosis pathway were dysregulated (Figure 2E). The mRNA expression of selected pro-apotopic and anti-apoptotic genes was again confirmed by qRT-PCR (Figure 2F). These results suggest that IAV induced cell death is mediated-through type I interferons, pro-inflammatory cytokines, and caspases and is IFI16-dependent.

IFI16 induces type I interferon and pro-inflammatory cytokines during IAV infection

We noticed that apart from upregulating apoptotic genes, knocking down IFI16 also downregulates interferon signaling and pro-inflammatory cytokine production pathways during IAV infection (Figures 3A, 3B, and S3A). Previous studies have shown that IAV infection activates apoptosis and pyroptosis by triggering PRR induced gene expression of pro-inflammatory cytokines and type I interferons and type I interfero ns-inducible genes. Therefore, to further investigate which of these pathways are involved in IAV induced cell death, we used pharmacological inhibitors to pyroptosis and necroptosis pathways, Z-VAD-FMK, a pan-caspase inhibitor, and necrostatin-1, respectively. Only Z-VAD-FMK but not necrostatin-1 could inhibit cell death, indicating that IAV induces cell death through pyroptosis (Figure S3B). Necrostatin-1 could not inhibit cells death, probably because necroptosis is repressed in A549 cells as it lacks a crucial component of necroptosis, RIPK3 (Gaba et al., 2019; Koo et al., 2015). In addition, we could not find much difference between shIFI16 cells and shSCR cells treated with Z-VAD after infecting

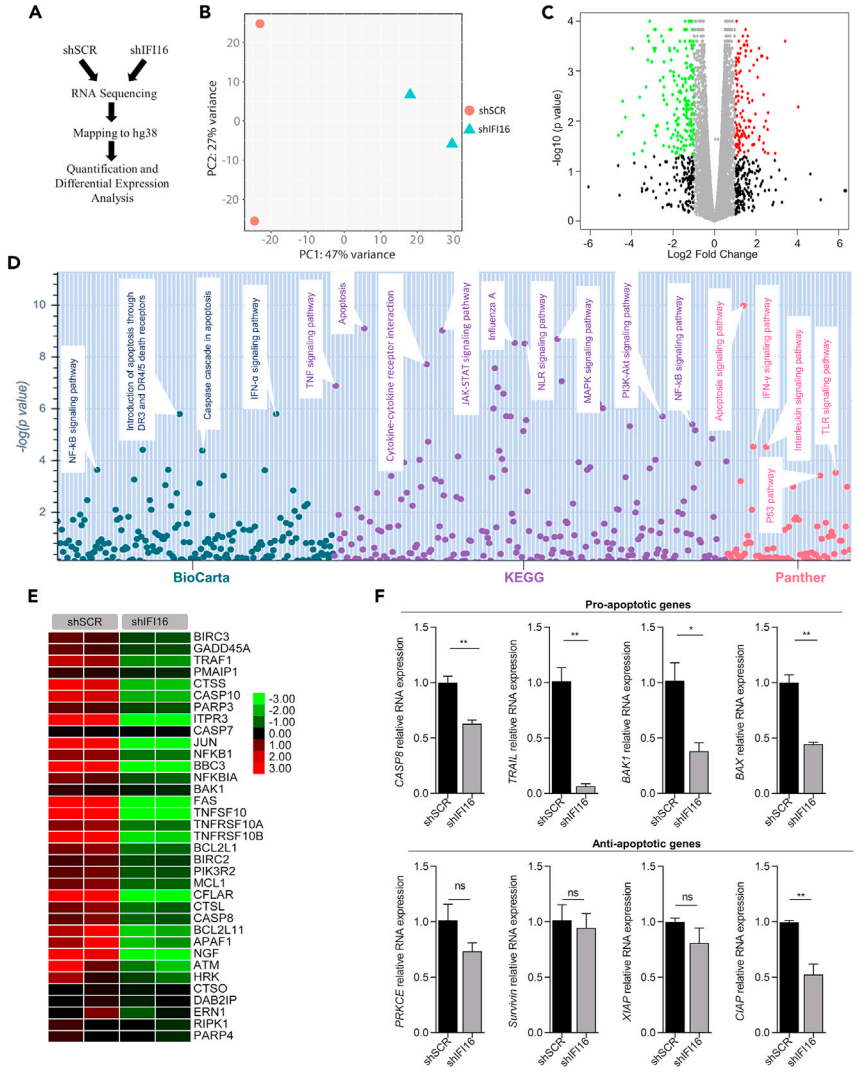

Figure 2. IFI16 induce programmed cell death in IAV infected cells

(A) A schematic representation of RNA-Sequencing data analysis.

(B) Principal component analysis of samples resulted in the formation of two distinct groups (shSCR and shIFI16, in duplicates) according to their treatment.

(C) Volcano plot showing differentially expressed genes in shIFI16 group.

(D) Pathway analysis of significantly upregulated genes using Biocarta_16, KEGG_2019_human, and Panther_2016 database.

(E) Heatmap showing expression of genes associated with apoptosis pathways in different samples.

(F) mRNA expression of selected pro-apotopic and anti-apoptotic genes was again confirmed by qRT-PCR. Data are mean ± SEMs from triplicate samples of a single experiment and are representative of results from three independent experiments. ****, $p < 0.0001$, ***, $p < 0.001$, **, $p < 0.01$, and *, $p < 0.05$, by two-tailed unpaired t test (F). ns, nonsignificant.

with IAV, indicating that IAV induced pyroptotic cell death in an IFI16 dependent manner (Figure 3C). Furthermore, the expression of the pyroptosis inducing cysteine proteases, caspase-1 and caspase-3, was significantly reduced in shIFI16 cells compared to shSCR (Figure 3D). Activation of caspase-1 was analyzed by FAM-FLICA caspase-1 assay and was found to be less in shIFI16 cells, which confirms the requirement of IFI16 and type-I interferon signaling in the activation of pyroptosis during IAV infection (Figure 3E). We found that this phenomenon is specific to IAV, and IFI16 is dispensable for activating and releasing cytokines in response to other RNA virus infections (NDV) (Figures S3C–S3E). These data suggest a unique, type-I interferon and IFI16 dependent pathway of pyroptosis activation upon

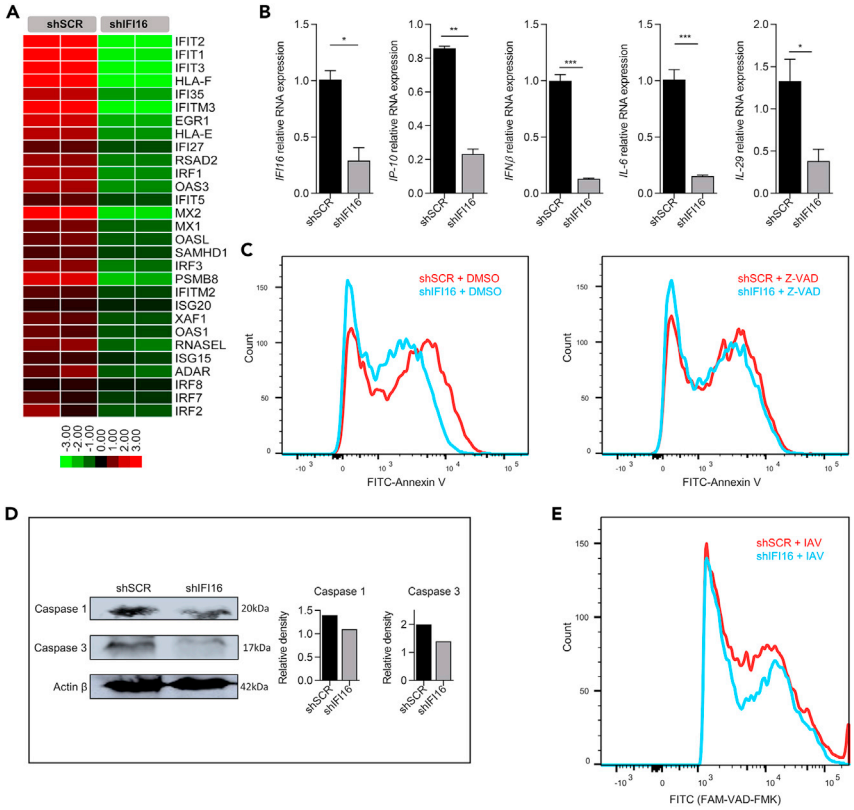

Figure 3. IFI16 induces type I interferon and pro-inflammatory cytokines during IAV infection

(A) Heatmap showing expression of interferon stimulated genes (ISGs) during IAV infection in different samples.

(B) mRNA expression of interferons, ISGs, and pro-inflammatory cytokines was again confirmed by qRT-PCR.

(C) A549 cells were transiently transfected with 2.0 μg of scrambled control (shSCR) for 48 h. shSCR and shIFI16 were treated with either DMSO or Z-VAD FMK (Z-VAD) for one hour before infection and then infected with IAV (MOI 10) for 24 h. Cells were then stained with annexin V and analyzed using flow cytometry for determination of apoptosis.

(D) Western blot analysis of Caspase 1 and Caspase 3 in shSCR and shIFI16 groups post IAV infection.

(E) FAM-FLICA caspase 1 assay was performed to check the activation of caspase 1, and analysis was done through flow cytometry. Data are mean ± SEMs from triplicate samples of a single experiment and are representative of results from three independent experiments. ****, $p < 0.0001$, ***, $p < 0.001$, **, $p < 0.01$, and *, $p < 0.05$, by two-tailed unpaired t test (B). ns, nonsignificant.

IAV infection, which was not previously reported. To determine the main driving factor for cell death, cytokines, or viral RNA replication, we examined the potential paracrine-signaling effects on cell death induction in uninfected cells using a transwell culture system. As shown in the representative figure (Figure S4A), cells were either mock-infected in both compartments or were infected with IAV only in the top compartment; the transwell culture system only allows paracrine signaling factors to move across. Upper compartments were removed 24 h postinfection, and cell viability in the lower compartment was measured using Annexin-V staining. Cells infected in the top compartment did not induce cell death in uninfected cells in the lower compartment, indicating that paracrine-signaling is not associated with IAV-induced cell death. Conversely, pretreatment of infected cells with the RNA polymerase II and viral RNA-dependent RNA polymerase (RdRp) inhibitor actinomycin-D suppressed the cell death (Figure S4B), and UV irradiation of IAV before infection also significantly reduced cell death (Figure S4C) in proportion to the reduction in the virus infectivity. Altogether, these results suggest that cell death induction involves both extrinsic and intrinsic mechanisms and likely requires virus RNA replication.

IFI16 interacts with IAV RNA to restrict its replication

IFI16 is known to sense cytosolic DNA from various DNA viruses and intracellular bacteria. However, it is not clear if it plays any role during IAV infection. To find if IFI16 interacts with IAV RNA, we performed RNA-immunoprecipitation (RNA-IP) of Flag-tagged IFI16 protein using anti-flag antibody, viral RNA in the precipitate was

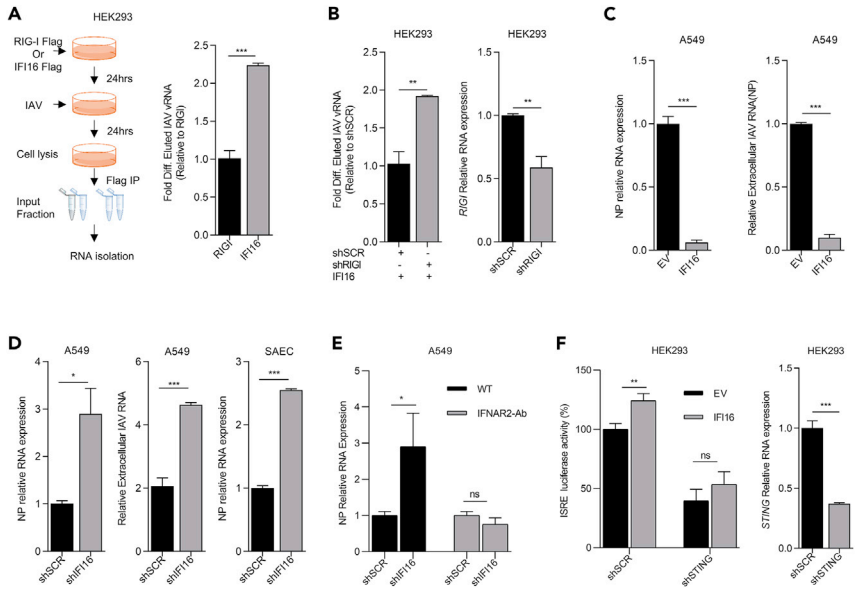

Figure 4. IFI16 interacts with IAV RNA to restrict its replication

(A) Schematic for RNA immunoprecipitation (RNA-IP) (left side). 2.0 μg of Flag-tagged IFI16 and RIG-I were overexpressed in HEK293T cells and then infected with IAV (MOI 10) for 24 h. RNA-IP was performed using Anti-flag M2 Affinity gel, and viral RNA in the precipitate was analyzed by qRT-PCR using Input RNA for normalization. Fold differences in viral RNA levels relative to RIG-I were determined using the following equation: $2 - \Delta\Delta Ct = [(Ct\ sample\ pulldown - Ct\ sample\ input)] - [(Ct\ RIG-I\ pulldown - Ct\ RIG-I\ input)$.

(B) RIGI knocked down cells were overexpressed with IFI16 or EV and infected with IAV (10MOI) for 24 h. RNA-IP was performed using Anti-flag M2 Affinity gel, and viral RNA in the precipitate was analyzed by qRT-PCR using Input RNA for normalization.

(C) A549 cells were transfected with plasmid expressing IFI16 or the empty vector backbone (EV) and infected with IAV (MOI 10) for 24 h. Relative NP RNA was measured in total RNA (Left panel) and extracellular RNA (Right panel) by qRT-PCR. NP RNA expression was normalized to mock infected samples.

(D) A549 and SAEC cells were transiently transfected with 2.0 μg of shIFI16 or scrambled control plasmids for 48 h then infected with IAV (MOI 10). Relative NP RNA in the total RNA was analyzed by qRT-PCR.

(E) A549 and SAEC cells were transiently transfected with 2.0 μg of shIFI16 or scrambled control plasmids for 48 h. Before infection, cells were treated with anti-IFNAR2 antibody and then infected with IAV (MOI 10). Relative NP RNA in the total RNA was analyzed by qRT-PCR.

(F) STING knocked down cells were over expressed with IFI16 or EV along with ISRE promoter containing luciferase construct and infected with IAV (10MOI) for 24 h. ISRE promoter activity was measured by luciferase assay. Data are mean ± SEMs from triplicate samples of a single experiment and are representative of results from three independent experiments. ****, $p < 0.0001$, ***, $p < 0.001$, **, $p < 0.01$, and *, $p < 0.05$, by two-tailed unpaired t test (A to F). ns, nonsignificant.

analyzed by RT-PCR. IAV RNA was present in the anti-Flag pulldown, and surprisingly, the enrichment of IAV RNA was orders of magnitude greater than of RIG-I, a well-known sensor of IAV, despite similar levels of IAV RNA in the input (Figures 4A and S4D). To eliminate the involvement of RIG-I targeting IAV RNA, we overexpressed IFI16 in RIG-I knocked down cells. Interestingly, RIG-I knockdown increased IAV RNA binding with IFI16, indicating that both RIG-I and IFI16 compete to interact with the same target (IAV RNA) (Figure 4B).

Next, we asked if the sensing of IAV RNA by IFI16 has any effects on IAV replication; overexpression of IFI16 led to a decrease in IAV RNA inside cells as well as in supernatant (Figure 4C) and knockdown of IFI16 led to an increase in IAV infection (Figure 4D) in both A549 and in primary small airway epithelial cells (SAEC). To confirm that IFI16 restricts viral infection by eliciting type I interferon signaling, we blocked type I interferon receptor (IFNAR2) by antibody and found that silencing type I interferon signaling abolished the effect of IFI16 on IAV replication (Figures 4E, S4E, and S4F). IFI16 is reported to sense DNA and initiate TBK-1-dependent IFNβ production via an adaptor STING. Therefore, to analyze the involvement of downstream STING-TBK1 axis in IFI16 mediated IAV sensing, we overexpressed IFI16 and ISRE promoter reporter plasmid in STING knockdown cells and analyzed

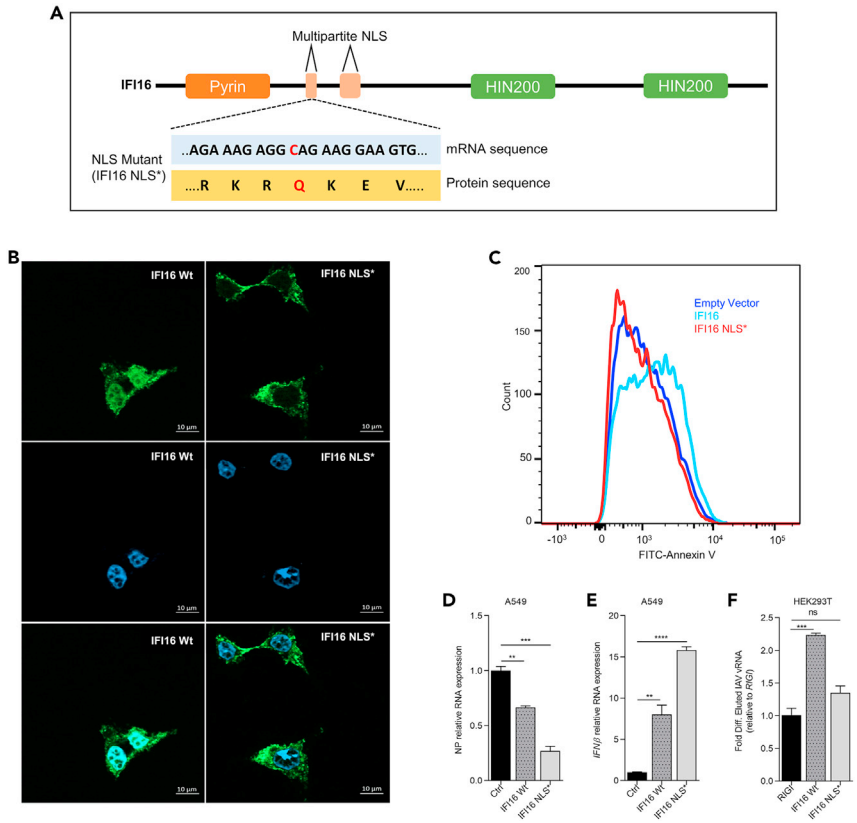

Figure 5. Intracellular localization of IFI16 is essential in restraining infection

(A) Schematic showing the multipartite Nuclear Localization Signal (NLS) sequence of IFI16. The mutation made in the NLS sequence is marked in red.

(B) GFP-tagged IFI16 and NLS mutant of IFI16 (IFI16 NLS*) were overexpressed in HEK293T cells. Cells were observed under a Microscope to find the IFI16 localization.

(C) A549 cells were transfected with IFI16 Wt and IFI16 NLS* and infected with IAV (MOI 10) for 24 h. Cells were then stained with annexin V and analyzed using flow cytometry for determination of apoptosis.

(D and E) Relative expression of NP and IFNβ RNAs were measured in total RNA by qRT-PCR.

(F) Flag-tagged IFI16 Wt, IFI16 NLS*, and RIG-I were overexpressed in HEK293T cells and then infected with IAV (MOI 10) for 24 h. RNA-IP was performed using Anti-flag M2 Affinity gel, and expression of viral RNA in the IP-ied sample was analyzed by qRT-PCR using Input RNA for normalization. Fold differences in viral RNA levels relative to RIG-I were determined using the following equation: $2 - \Delta\Delta Ct = [(Ct\ sample\ pulldown - Ct\ sample\ input)] - [(Ct\ RIG-I\ pulldown - Ct\ RIG-I\ input)$. Data are mean ± SEMs from triplicate samples of a single experiment and are representative of results from three independent experiments. ****, $p < 0.0001$, ***, $p < 0.001$, **, $p < 0.01$, and *, $p < 0.05$, by two-tailed unpaired t test (D–F). ns, nonsignificant.

luciferase activity. Results of ISRE promoter reporter assays after IAV infection confirm that STING is a necessary adaptor for signal transduction when IFI16 senses IAV RNA (Figure 4F).

Nuclear and cytoplasmic localization of IFI16 is essential in restraining infection and sensing IAV genomic RNA

To test the effect of IFI16's subcellular localization on its viral RNA sensing, we mutated nuclear localization sequences (NLS) on the N-terminus of the IFI16 (Figure 5A). NLS mutation was able to restrict most of the (>70%) IFI16 protein to the cytosol (Figure 5B). Cells expressing IFI16-NLS mutant were more resistant to IAV induced cell death than cells expressing an equivalent amount of WT-IFI16 (Figure 5C). In addition, IAV infection was less and IFNβ was more in cells expressing IFI16-NLS mutant than the cells expressing WT-IFI16 (Figures 5D and 5E). In contrast, cells expressing WT-IFI16 showed more IAV-RNA than cells expressing an equal amount of IFI16-NLS mutant when IFI16 was pulled down using anti-flag antibody

(Figure 5F). Previous reports suggest that IFI16 binds to viral DNA through two tandem repeats of hematopoietic interferon-inducible nuclear (HINa, HINb) domains and one pyrin domain. We made multiple IFI16 mutants lacking either pyrin, HINa, HINb, or both HIN domains. IFI16 mutant having just the HINb domain was found to restrict viral infection similar to wild type IFI16, indicating a significant role of HINb domain (Figures S5A and S5B). Collectively, these data suggest that IFI16 is recruited into the nucleus of infected cells, where it interacts with IAV-RNA and initiates inflammatory cell death responses. We also found that only IFI16, among other members of ALR's (AIM2-like receptors), plays a vital role in the regulation of Influenza virus infection (Figure S5C).

DISCUSSION

PRRs sense conserved structures on invading pathogens and deploy various cellular and molecular components in antimicrobial response. Although our understanding of the innate immune system has exponentially increased in the past few decades, several questions such as, how a limited number of germline-encoded PRRs orchestrate an array of immune responses against the spectrum of pathogens remains the most perplexing enigma in innate immunobiology. This report demonstrates that a single PRR can elicit an immune response against different classes of pathogen origin molecular patterns. IFI16 is a key viral restriction factor against DNA viruses. Upon sensing viral DNA, it induces pro-inflammatory cytokines through ASC-dependent inflammasome pathway and IFNβ through STING-TBK1-IRF3 signaling axis. We have demonstrated that IFI16 interacts with IAV genomic RNA and restricts viral infection. Recently an independent group reported that IFI16 binds with IAV viral RNA (Jiang et al., 2021). In addition, we also demonstrated that upon interacting with the IAV genomic RNA, it induces IFI16-dependent programmed cell death to eliminate infected cells. In humans and other mammals, respiratory epithelial cells are the primary target of IAV infection, where a lytic virus replicates in dying infected cells, causing desquamation in the respiratory tract of the host. Controlled, programmed cell death could be an effective host defense mechanism that suppresses cell-to-cell viral transmission, and subsequently, virus infection. Despite such an important host antiviral response, the exact molecular details driving programmed cell death upon viral infection remain unclear.

Caspase-1-dependent pyroptosis has been shown in respiratory and primary bronchial epithelial cells in *in vitro* conditions, and similar exaggerated inflammatory response and cell death were also reported upon IAV infection *in vivo*. Our study has now identified a unique role of IFI16-mediated sensing of the viral RNA; it induces cell death in the form of apoptosis and pyroptosis. Another recent study has shown the RNA binding ability of IFI16 during Togaviridae family member, Chikungunya virus (CHIKV) infection, where IFI16 was found to restrict viral replication by binding to genomic RNA. In agreement with this, we found that IFI16 can bind to IAV genomic RNA as well. The two tandem repeats of hematopoietic interferon-inducible nuclear (HIN) domains of IFI16 are known to bind foreign DNA. Our results demonstrate that IAV RNA sensed by the IFI16 requires active replication of the virus in the nucleus. Consistent with previous findings of its DNA sensing ability, it indicates that the same domains that bind DNA can also bind RNA. Although the exact molecular mechanism of how a DNA sensing protein is binding to the RNA needs further investigation, this demonstrates the multi-role of PRRs in combating different types of virus infection.

Emerging RNA virus infections pose a significant threat to the socio-economic status of humankind. Finding drugs or vaccines for these emerging pathogens is highly challenging because of their high mutation rates. The ongoing Coronavirus pandemic associated vaccine and therapeutic discovery is a perfect example of this challenge. However, the mechanism of viral pathogenesis and innate immune strategies to block viral infection can pave the way for finding potential druggable targets. In this study, we provide evidence for the contribution of IFI16, a DNA sensor in sensing RNA from IAV and its downstream signaling results to cell death, suggesting that the multi-layer sensing system of IAV ensures all possible development of the appropriate and regulated antiviral state. Our study suggests IFI16, a member of ALR (AIM2-like receptors), as an innate immune sensor of IAV regulating antiviral responses. Insights gained from this study will improve our understanding of the mechanisms of regulation of IAV pathogenesis and lead to identifying more possible targets for therapeutic intervention.

Limitations of the study

The limitation of this study is that genetic study under physiological conditions is lacking.

STAR★METHODS

Detailed methods are provided in the online version of this paper and include the following:

- KEY RESOURCES TABLE
- RESOURCE AVAILABILITY
  - Lead contact
  - Material availability
  - Data and code availability
- EXPERIMENTAL MODEL AND SUBJECT DETAILS
- METHOD DETAILS
  - Analysis of microarray data from the GEO database
  - Cells, transfection, viruses, and reagents
  - Short hairpin (sh)RNA mediated transient knock-down
  - Generation of A/PR8/H1N1 virus
  - Cloning, plasmids, and site-directed mutagenesis
  - Trypan blue exclusion assay
  - Cell viability assay
  - Quantitative real-time reverse transcription-PCR
  - Fluorescence-activated cell sorting cytometry analysis
  - RNA-seq analysis
  - Enzyme-linked immunosorbent assay (ELISA)
  - Western blotting analysis
  - ImageJ image analysis
  - RNA immunoprecipitation
  - Caspase-1 assay
- QUANTIFICATION AND STATISTICAL ANALYSIS

SUPPLEMENTAL INFORMATION

Supplemental information can be found online at https://doi.org/10.1016/j.isci.2021.103714.

ACKNOWLEDGMENTS

We thank Professor David Knipe for providing us IFI16 plasmid, R. Fouchier for providing the A/PR8/H1N1 reverse genetics system, P. Palese for providing green fluorescent protein-expressing NDV (NDV-GFP), and Professor Yan Yuan for providing the pCMV3Tag1a plasmid. We also thank Dr. Ashwin Ashok Raut (NIHSAD, Bhopal) for initial amplification of PR8 virus in SPF eggs. We thank IISER Bhopal for providing the Central Instrumentation Facility. We are extremely thankful to Department of Biotechnology India (DBT)-(BT/PR25052/NER/95/983/2017), Science and Engineering Research Board, India (SERB)-(CRG/2020/001417) and IISER Bhopal for the funding.

AUTHOR CONTRIBUTIONS

Conceptualization, S.M. and H.K.; Investigation, S.M. and A.S.R.; Validation, S.M., A.S.R., A.K., A.R., and P.K.; Formal Analysis, S.M., A.S.R., and A.K.; Data Curation, S.M. and A.S.R.; Writing-Original Draft, S.M., A.S.R., and H.K.; Writing-Review and Editing, A.S.R., A.K., and H.K.; Project Administration, H.K.; Funding Acquisition, H.K.; Resources, H.K.; Supervision, H.K.

DECLARATION OF INTERESTS

The authors declare no competing interests.

Received: March 2, 2021
Revised: October 4, 2021
Accepted: December 29, 2021
Published: January 21, 2022

REFERENCES

Bolger, A.M., Lohse, M., and Usadel, B. (2014). Trimmomatic: a flexible trimmer for illumina sequence data. Bioinformatics *30*, 2114–2120. https://doi.org/10.1093/bioinformatics/btu170.

Carrasco-Hernandez, R., Jacome, R., Lopez Vidal, Y., and Ponce de Leon, S. (2017). Are RNA viruses candidate agents for the next global pandemic? A review. ILAR J. *58*, 343–358. https://doi.org/10.1093/ilar/ilx026.

Chen, W., Calvo, P.A., Malide, D., Gibbs, J., Schubert, U., Bacik, I., Basta, S., O'Neill, R., Schickli, J., Palese, P., et al. (2001). A novel influenza A virus mitochondrial protein that induces cell death. Nat. Med. *7*, 1306–1312. https://doi.org/10.1038/nm1201-1306.

Chung, W.C., Kang, H.R., Yoon, H., Kang, S.J., Ting, J.P., and Song, M.J. (2015). Influenza A virus NS1 protein inhibits the NLRP3 inflammasome. PLoS One *10*, e0126456. https://doi.org/10.1371/journal.pone.0126456.

de Wit, E., Spronken, M.I., Bestebroer, T.M., Rimmelzwaan, G.F., Osterhaus, A.D., and Fouchier, R.A. (2004). Efficient generation and growth of influenza virus A/PR/8/34 from eight cDNA fragments. Virus Res. *103*, 155–161. https://doi.org/10.1016/j.virusres.2004.02.028.

Duffy, S. (2018). Why are RNA virus mutation rates so damn high? PLoS Biol. *16*, e3000003. https://doi.org/10.1371/journal.pbio.3000003.

Gaba, A., Xu, F., Lu, Y., Park, H.S., Liu, G., and Zhou, Y. (2019). The NS1 protein of influenza A virus participates in necroptosis by interacting with MLKL and increasing its oligomerization and membrane translocation. J. Virol. *93*, e01835-18. https://doi.org/10.1128/JVI.01835-18.

Halder, U.C., Bagchi, P., Chattopadhyay, S., Dutta, D., and Chawla-Sarkar, M. (2011). Cell death regulation during influenza A virus infection by matrix (M1) protein: a model of viral control over the cellular survival pathway. Cell Death Dis. *2*, e197. https://doi.org/10.1038/cddis.2011.75.

Hansen, K., Prabakaran, T., Laustsen, A., Jorgensen, S.E., Rahbaek, S.H., Jensen, S.B., Nielsen, R., Leber, J.H., Decker, T., Horan, K.A., et al. (2014). Listeria monocytogenes induces IFNbeta expression through an IFI16-, cGAS- and STING-dependent pathway. EMBO J. *33*, 1654–1666. https://doi.org/10.15252/embj.201488029.

Iuliano, A.D., Roguski, K.M., Chang, H.H., Muscatello, D.J., Palekar, R., Tempia, S., Cohen, C., Gran, J.M., Schanzer, D., Cowling, B.J., et al. (2018). Estimates of global seasonal influenza-associated respiratory mortality: a modelling study. Lancet *391*, 1285–1300. https://doi.org/10.1016/S0140-6736(17)33293-2.

Jakobsen, M.R., Bak, R.O., Andersen, A., Berg, R.K., Jensen, S.B., Tengchuan, J., Laustsen, A., Hansen, K., Ostergaard, L., Fitzgerald, K.A., et al. (2013). IFI16 senses DNA forms of the lentiviral replication cycle and controls HIV-1 replication. Proc. Natl. Acad. Sci. U S A *110*, E4571–E4580. https://doi.org/10.1073/pnas.1311669110.

Jiang, Z., Wei, F., Zhang, Y., Wang, T., Gao, W., Yu, S., Sun, H., Pu, J., Sun, Y., Wang, M., et al. (2021). IFI16 directly senses viral RNA and enhances RIG-I transcription and activation to restrict influenza virus infection. Nat. Microbiol. *6*, 932–945. https://doi.org/10.1038/s41564-021-00907-x.

Kerur, N., Veettil, M.V., Sharma-Walia, N., Bottero, V., Sadagopan, S., Otageri, P., and Chandran, B. (2011). IFI16 acts as a nuclear pathogen sensor to induce the inflammasome in response to Kaposi sarcoma-associated herpesvirus infection. Cell Host Microbe *9*, 363–375. https://doi.org/10.1016/j.chom.2011.04.008.

Kesavardhana, S., Kuriakose, T., Guy, C.S., Samir, P., Malireddi, R.K.S., Mishra, A., and Kanneganti, T.D. (2017). ZBP1/DAI ubiquitination and sensing of influenza vRNPs activate programmed cell death. J. Exp. Med. *214*, 2217–2229. https://doi.org/10.1084/jem.20170550.

Koo, G.B., Morgan, M.J., Lee, D.G., Kim, W.J., Yoon, J.H., Koo, J.S., Kim, S.I., Kim, S.J., Son, M.K., Hong, S.S., et al. (2015). Methylation-dependent loss of RIP3 expression in cancer represses programmed necrosis in response to chemotherapeutics. Cell Res. *25*, 707–725. https://doi.org/10.1038/cr.2015.56.

Kumar, A., Kumar, A., Ingle, H., Kumar, S., Mishra, R., Verma, M.K., Biswas, D., Kumar, N.S., Mishra, A., Raut, A.A., et al. (2018). MicroRNA hsa-miR-324-5p suppresses H5N1 virus replication by targeting the viral PB1 and host CUEDC2. J. Virol. *92*, e01057-18. https://doi.org/10.1128/JVI.01057-18.

Kuriakose, T., Man, S.M., Malireddi, R.K., Karki, R., Kesavardhana, S., Place, D.E., Neale, G., Vogel, P., and Kanneganti, T.D. (2016). ZBP1/DAI is an innate sensor of influenza virus triggering the NLRP3 inflammasome and programmed cell death pathways. Sci. Immunol. *1*, aag2045. https://doi.org/10.1126/sciimmunol.aag2045.

Le Goffic, R., Pothlichet, J., Vitour, D., Fujita, T., Meurs, E., Chignard, M., and Si-Tahar, M. (2007). Cutting edge: influenza A virus activates TLR3-dependent inflammatory and RIG-I-dependent antiviral responses in human lung epithelial cells. J. Immunol. *178*, 3368–3372. https://doi.org/10.4049/jimmunol.178.6.3368.

Lee, S., Hirohama, M., Noguchi, M., Nagata, K., and Kawaguchi, A. (2018). Influenza A virus infection triggers pyroptosis and apoptosis of respiratory epithelial cells through the type I interferon signaling pathway in a mutually exclusive manner. J. Virol. *92*, e00396-18. https://doi.org/10.1128/JVI.00396-18.

Lei, Y., Moore, C.B., Liesman, R.M., O'Connor, B.P., Bergstralh, D.T., Chen, Z.J., Pickles, R.J., and Ting, J.P. (2009). MAVS-mediated apoptosis and its inhibition by viral proteins. PLoS One *4*, e5466. https://doi.org/10.1371/journal.pone.0005466.

Li, T., Chen, J., and Cristea, I.M. (2013). Human cytomegalovirus tegument protein pUL83 inhibits IFI16-mediated DNA sensing for immune evasion. Cell Host Microbe *14*, 591–599. https://doi.org/10.1016/j.chom.2013.10.007.

Li, T., Diner, B.A., Chen, J., and Cristea, I.M. (2012). Acetylation modulates cellular distribution and DNA sensing ability of interferon-inducible protein IFI16. Proc. Natl. Acad. Sci. U S A *109*, 10558–10563. https://doi.org/10.1073/pnas.1203447109.

Liu, G., Park, H.S., Pyo, H.M., Liu, Q., and Zhou, Y. (2015). Influenza A virus panhandle structure is directly involved in RIG-I activation and interferon induction. J. Virol. *89*, 6067–6079. https://doi.org/10.1128/JVI.00232-15.

Love, M.I., Huber, W., and Anders, S. (2014). Moderated estimation of fold change and dispersion for RNA-seq data with DESeq2. Genome Biol. *15*, 550. https://doi.org/10.1186/s13059-014-0550-8.

Martinez-Sobrido, L., and Garcia-Sastre, A. (2010). Generation of recombinant influenza virus from plasmid DNA. J. Vis. Exp. *10*, 2057. https://doi.org/10.3791/2057.

Moriyama, M., Chen, I.Y., Kawaguchi, A., Koshiba, T., Nagata, K., Takeyama, H., Hasegawa, H., and Ichinohe, T. (2016). The RNA- and TRIM25-binding domains of influenza virus NS1 protein are essential for suppression of NLRP3 inflammasome-mediated interleukin-1beta secretion. J. Virol. *90*, 4105–4114. https://doi.org/10.1128/JVI.00120-16.

Mosavi, S.Z., Shahsavandi, S., Ebrahimi, M.M., Hatami, A.R., Sadeghi, K., and Shahivandi, H. (2015). Necrotic response to low pathogenic H9N2 influenza virus in chicken hepatoma cells. Jundishapur J. Microbiol. *8*, e13770. https://doi.org/10.5812/jjm.13770.

Orzalli, M.H., DeLuca, N.A., and Knipe, D.M. (2012). Nuclear IFI16 induction of IRF-3 signaling during herpesviral infection and degradation of IFI16 by the viral ICP0 protein. Proc. Natl. Acad. Sci. U S A *109*, E3008–E3017. https://doi.org/10.1073/pnas.1211302109.

Rozen, R., Sathish, N., Li, Y., and Yuan, Y. (2008). Virion-wide protein interactions of Kaposi's sarcoma-associated herpesvirus. J Virol *82*, 4742–4750. https://doi.org/10.1128/JVI.02745-07.

Sanders, C.J., Vogel, P., McClaren, J.L., Bajracharya, R., Doherty, P.C., and Thomas, P.G. (2013). Compromised respiratory function in lethal influenza infection is characterized by the depletion of type I alveolar epithelial cells beyond threshold levels. Am. J. Physiol. Lung Cell Mol. Physiol. *304*, L481–L488. https://doi.org/10.1152/ajplung.00343.2012.

Sathish, N., Zhu, F.X., and Yuan, Y. (2009). Kaposi's sarcoma-associated herpesvirus ORF45 interacts with kinesin-2 transporting viral capsid-tegument complexes along microtubules. PLoS Pathog. *5*, e1000332. https://doi.org/10.1371/journal.ppat.1000332.

Singh, V.V., Kerur, N., Bottero, V., Dutta, S., Chakraborty, S., Ansari, M.A., Paudel, N., Chikoti, L., and Chandran, B. (2013). Kaposi's sarcoma-associated herpesvirus latency in endothelial and B cells activates gamma interferon-inducible protein 16-mediated inflammasomes. J. Virol. *87*, 4417–4431. https://doi.org/10.1128/JVI.03282-12.

Stasakova, J., Ferko, B., Kittel, C., Sereinig, S., Romanova, J., Katinger, H., and Egorov, A. (2005). Influenza A mutant viruses with altered NS1 protein function provoke caspase-1 activation in primary human macrophages, resulting in fast apoptosis and release of high levels of interleukins 1beta and 18. J. Gen. Virol. *86*, 185–195. https://doi.org/10.1099/vir.0.80422-0.

Thapa, R.J., Ingram, J.P., Ragan, K.B., Nogusa, S., Boyd, D.F., Benitez, A.A., Sridharan, H., Kosoff, R., Shubina, M., Landsteiner, V.J., et al. (2016). DAI senses influenza A virus genomic RNA and activates RIPK3-dependent cell death. Cell Host Microbe *20*, 674–681. https://doi.org/10.1016/j.chom.2016.09.014.

Thomas, P.G., Dash, P., Aldridge, J.R., Jr., Ellebedy, A.H., Reynolds, C., Funk, A.J., Martin, W.J., Lamkanfi, M., Webby, R.J., Boyd, K.L., et al. (2009). The intracellular sensor NLRP3 mediates key innate and healing responses to influenza A virus via the regulation of caspase-1. Immunity *30*, 566–575. https://doi.org/10.1016/j.immuni.2009.02.006.

Thompson, M.R., Sharma, S., Atianand, M., Jensen, S.B., Carpenter, S., Knipe, D.M., Fitzgerald, K.A., and Kurt-Jones, E.A. (2014). Interferon gamma-inducible protein (IFI) 16 transcriptionally regulates type i interferons and other interferon-stimulated genes and controls the interferon response to both DNA and RNA viruses. J. Biol. Chem. *289*, 23568–23581. https://doi.org/10.1074/jbc.M114.554147.

Thompson, W.W., Shay, D.K., Weintraub, E., Brammer, L., Cox, N., Anderson, L.J., and Fukuda, K. (2003). Mortality associated with influenza and respiratory syncytial virus in the United States. JAMA *289*, 179–186. https://doi.org/10.1001/jama.289.2.179.

Tripathi, S., Batra, J., Cao, W., Sharma, K., Patel, J.R., Ranjan, P., Kumar, A., Katz, J.M., Cox, N.J., Lal, R.B., et al. (2013). Influenza A virus nucleoprotein induces apoptosis in human airway epithelial cells: implications of a novel interaction between nucleoprotein and host protein clusterin. Cell Death Dis. *4*, e562. https://doi.org/10.1038/cddis.2013.89.

Unterholzner, L., Keating, S.E., Baran, M., Horan, K.A., Jensen, S.B., Sharma, S., Sirois, C.M., Jin, T., Latz, E., Xiao, T.S., et al. (2010). IFI16 is an innate immune sensor for intracellular DNA. Nat. Immunol. *11*, 997–1004. https://doi.org/10.1038/ni.1932.

Webster, R.G., Laver, W.G., Air, G.M., and Schild, G.C. (1982). Molecular mechanisms of variation in influenza viruses. Nature *296*, 115–121. https://doi.org/10.1038/296115a0.

Wichit, S., Hamel, R., Yainoy, S., Gumpangseth, N., Panich, S., Phuadraksa, T., Saetear, P., Monteil, A., Morales Vargas, R., and Misse, D. (2019). Interferon-inducible protein (IFI) 16 regulates Chikungunya and Zika virus infection in human skin fibroblasts. EXCLI J. *18*, 467–476. https://doi.org/10.17179/excli2019-1271.

Zamarin, D., Garcia-Sastre, A., Xiao, X., Wang, R., and Palese, P. (2005). Influenza virus PB1-F2 protein induces cell death through mitochondrial ANT3 and VDAC1. PLoS Pathog. *1*, e4. https://doi.org/10.1371/journal.ppat.0010004.

Zhai, A., Qian, J., Kao, W., Li, A., Li, Y., He, J., Zhang, Q., Song, W., Fu, Y., Wu, J., et al. (2013). Borna disease virus encoded phosphoprotein inhibits host innate immunity by regulating miR-155. Antivir. Res. *98*, 66–75. https://doi.org/10.1016/j.antiviral.2013.02.009.

STAR★METHODS

KEY RESOURCES TABLE

REAGENT or RESOURCE	SOURCE	IDENTIFIER
Antibodies		
Mouse monoclonal anti-IFI16	Santa Cruz Biotechnology	sc-8023; RRID:AB_627775
Mouse monoclonal anti-Flag	Sigma Aldrich	F1804; RRID:AB_262044
Rabbit Polyclonal anti-Caspase-3	Cell Signaling Technology	#9662; RRID:AB_331439
Rabbit Monoclonal anti-Caspase-1	Cell Signaling Technology	#4199; RRID:AB_1903916
Mouse Monoclonal anti-β actin	Sigma Aldrich	A1978; RRID:AB_476692
Rabbit polyclonal anti-γ Tubulin	Sigma Aldrich	T5192; RRID:AB_261690
Bacterial and virus strains		
A/PR8/H1N1	R. Fouchier	N/A
NDV GFP	P. Palese	N/A
Chemicals, peptides, and recombinant proteins		
Z-VAD(OMe)-FMK	Santa Cruz Biotechnology	sc-311561
Necrostatin-1	Santa Cruz Biotechnology	sc-200142
Critical commercial assays		
FAM-FLICA	Immunochemistry Technologies	#97
Molecular Probes, Death Cell Apoptosis kit with Annexin V FITC and PI	Thermofisher Scientific	V13242
ANTI-FLAG® M2 Affinity Gel	Sigma Aldrich	A2220
Deposited data		
RNA seq	NCBI GEO	GSE163705
Experimental models: cell lines		
A549	NCCS	N/A
HEK293T	ATCC	CRL-3216
Oligonucleotides		
shRNA	Sigma Aldrich	MISSION®shRNA
18S Forward 5′-CTGCTTTCCTCAACACCACA-3′ Reverse 5′-ATCCCTGAAAAGTTCCAGCA-3′	This Paper	N/A
IFI16 Forward 5′-ACTCCTGGAGCTCAGAACCC-3′ Reverse 5′-CTGTGTCTGTGTAGCCACTGT-3′	This Paper	N/A
PR8 NP Forward 5′-GGAGGGGTGAGAATGGACGA-3′ Reverse 5′-GTCCATACACACAGGCAGGC-3′	This Paper	N/A
NDV Forward 5′-GGAGGATGTTGGCAGCATT-3′ Reverse 5′-GTCAACATATACACCTCATC-3′	This Paper	N/A
IFNβ Forward 5′-AGCTGCAGCAGTTCCAGAAG-3′ Reverse 5′-AGTCTCATTCCAGCCAGTGC-3′	This Paper	N/A
IL-6 Forward 5′-CTCAGCCCTGAGAAAGGAGA-3′ Reverse 5′-CCAGGCAAGTCTCCTCATTG-3′	This Paper	N/A

(*Continued on next page*)

Continued

REAGENT or RESOURCE	SOURCE	IDENTIFIER
IP-10 Forward 5′-TGGCATTCAAGGAGGTACCTCTC-3′ Reverse 5′-TGATCTCAACACGTGGACAAA-3′	This Paper	N/A
CASP8 Forward 5′-AGAGTCTGTGCCCAAATCAAC-3′ Reverse 5′-GCTGCTTCTCTCTTTGCTGAA-3′	This Paper	N/A
BAX Forward 5′-TCCCCCCGAGAGGTCTTTT-3′ Reverse 5′-CGGCCCCAGTTGAAGTTG-3′	This Paper	N/A
BAK Forward 5′-CATCAACCGACGCTATGACTC-3′ Reverse 5′-GTCAGGCCATGCTGGTAGAC-3′	This Paper	N/A
PRKCE Forward 5′-CAACGGACGCAAGATCGAG-3′ Reverse 5′-CTGGCTCCAGATCAATCCAGT-3′	This Paper	N/A
XIAP Forward 5′-TTTGCCTTAGACAGGCCATC-3′ Reverse 5′-TTTCCACCACAACAAAAGCA-3′	This Paper	N/A
Survivin Forward 5′-AGAACTGGCCCTTCTTGGAGG -3′ Reverse 5′-CTTTTTATGTTCCTCTATGGGGTC-3′	This Paper	N/A
cIAP1 Forward 5′-AGCTAGTCTGGGATCCACCTC-3′ Reverse 5′-GGGGTTAGTCCTCGATGAAG-3′	This Paper	N/A
TRAIL Forward 5′-AGCAATGCCACTTTTGGAGT-3′ Reverse 5′-TTCACAGTGCTCCTGCAGTC-3′	This Paper	N/A
IFI16 NLS SDM Forward 5′-GAGGCAGAAGGAAGTGGATGCT ACTTCACC-3′ Reverse 5′-CCTTCTGCCTCTTTCTTGATAGGGCTGG-3′.	This Paper	N/A
Recombinant DNA		
IFI16 Myc Plasmid	Professor David Knipe	Orzalli et al. (2012) https://doi.org/10.1073/pnas.1211302109
pCMV3Tag1a (FLAG)	Professor Yan Yuan, University of Pennsylvania	(Rozen et al., 2008) https://doi.org/10.1128/JVI.02745-07
Software and algorithms		
Flowjo	Flowjo	https://www.flowjo.com/
ImageJ	ImaeJ	https://imagej.nih.gov/ij/
Prism	Graphpad	https://www.graphpad.com/

RESOURCE AVAILABILITY

Lead contact

Further information and requests for resources and reagents should be directed to and will be fulfilled by the Lead Contact, Himanshu Kumar (hkumar@iiserb.ac.in).

Material availability

This study did not generate any unique reagent/s.

Data and code availability

Data: RNA-Seq data have been submitted to the Gene Expression Omnibus (NCBI-GEO) database under accession number (GSE163705). Any additional information required to reanalyze the data reported in this paper is available from the lead contact upon request.

Code: This paper does not report original code.

EXPERIMENTAL MODEL AND SUBJECT DETAILS

Cell lines: HEK293T (ATCC, CRL-3216), A549 (received from National Center for Cell Sciences, NCCS, Pune, India) and were cultured in DMEM media supplemented with 10% FBS (Gibco) and 1X antibiotic-antimycotic (Gibco) in 5% CO2 incubator at 37°C.

Virus strains: A/PR8/H1N1 (received from Dr. R. Fouchier), NDV-GFP (received from Dr. P. Palese).

METHOD DETAILS

Analysis of microarray data from the GEO database

Influenza H1N1 infected cell line and patient microarray data were obtained from the GEO database (GSE37571, GSE50628, GSE48466, GSE40844). Differentially expressed genes in the above datasets between mock-infected and H1N1 infected or Healthy and Patients were identified using the GEO2R online tool. Differentially expressed genes were plotted using various R packages.

Cells, transfection, viruses, and reagents

A549 human alveolar basal epithelial cells (Cell Repository, NCCS, India) and HEK293T human embryonic kidney cells (ATCC CRL-3216) were cultured in Dulbecco's modified Eagle's medium (DMEM) supplemented with 10% Fetal Bovine Serum (FBS) and 1% penicillin-streptomycin. Small airway epithelial cells (SAECs; Lonza) were cultured and maintained according to the manufacturer's instruction. Transfection of DNA and Poly(I-C) (InvivoGen) was performed with Lipofectamine 3000 (Invitrogen) in Opti-MEM as per the manufacturer's protocol. Cells were infected in serum-free DMEM with the A/Puerto Rico/8/34 (PR8/H1N1), or NDV Lasota viruses at the MOIs mentioned in the figure legends. After one hour, cells were washed with Phosphate buffered saline (PBS) and replaced with DMEM containing 1% FBS. DMEM, FBS, Opti-MEM, and penicillin-streptomycin were purchased from Invitrogen (Carlsbad, CA, USA).

Anti-FLAG, anti-β actin, and anti-γ Tubulin antibodies were purchased from Sigma Aldrich (St. Louis, MO, USA). Anti-Caspase-3 and Anti-Caspase-1 antibodies were purchased from Cell Signaling Technology (Danvers, MA, USA). The anti-IFI16 antibody was purchased from Santa Cruz Biotechnology (Dallas, TX, USA). IR dye-labelled anti-Rabbit and anti-Mouse IgG (secondary antibody) were purchased from LI-COR.

Short hairpin (sh)RNA mediated transient knock-down

shRNA clones were obtained from the whole RNAi human library for shRNA mediating silencing (Sigma, Aldrich) maintained at IISER, Bhopal, India. Cells were transfected with either control scrambled (scr) shRNA or specific shRNA clones against IFI16, IPS-1, STING, and MyD88 using Lipofectamine 3000 (Invitrogen) in Opti-MEM as per the manufacturer's protocol. The efficacy of each shRNA clone to downregulate the endogenous expression of IFI16, IPS-1, STING, and MyD88 in respective clones was measured by either semi-quantitative PCR or immunoblot.

Generation of A/PR8/H1N1 virus

A/PR8/H1N1 viruses were generated using eight plasmid system (de Wit et al., 2004; Kumar et al., 2018; Martinez-Sobrido and Garcia-Sastre, 2010). The eight plasmids were transfected in a coculture of MDCK (Madin-Darby Canine Kidney) and HEK293T cells which were cultured in DMEM supplied with 10% FBS. After 48hrs the supernatant containing virus was overlaid on MDCK or inoculated in 10 day old embroyonated eggs to further amplify viral titers.

Cloning, plasmids, and site-directed mutagenesis

pCMV3Tag1a (FLAG) was a kind gift from Professor Yan Yuan, University of Pennsylvania, Philadelphia. IFI16 plasmid was a kind gift from Professor Davide knipe. IFI16 was subcloned into PCMV 3tag1a for

tagging with flag and in PEGFP N1 for tagging with GFP. The NLS mutant of IFI16 was made by site-directed mutagenesis using the primers 5′-GAGGCAGAAGGAAGTGGATGCTACTTCACC-3′ 5′-CCTT CTGCCTCTTTCTTGATAGGGCTGG-3′.

Trypan blue exclusion assay

Cells were treated stained with Trypan blue and counted stained (dead) and unstained (live)cells using a hemocytometer.

Cell viability assay

MTT [3-(4,5-dimethylthiazol-2-yl)-2,5- diphenyl tetrazolium bromide] assay was performed by treating it with cells and counting the viable cells under microscope using hemocytometer (Lei et al., 2009).

Quantitative real-time reverse transcription-PCR

Total RNA was isolated using TRIzol reagent (Ambion/Invitrogen) and was used to prepare cDNA using is-cript cDNA synthesis kit (Bio-Rad) following the manufacturer's protocol. Gene expression was estimated by quantitative real-time PCR using SYBR green chemistry (Bio-Rad) and gene-specific primers18S (5′-CT GCTTTCCTCAACACCACA-3′ 5′-ATCCCTGAAAAGTTCCAGCA-3′)

IFI16 (5′-ACTCCTGGAGCTCAGAACCC-3′ 5′-CTGTGTCTGTGTAGCCACTGT-3′)

PR8 NP (5′-GGAGGGGTGAGAATGGACGA-3′ 5′-GTCCATACACACAGGCAGGC-3′)

NDV (5′-GGAGGATGTTGGCAGCATT-3′ 5′-GTCAACATATACACCTCATC-3′)

IFNβ (5′-AGCTGCAGCAGTTCCAGAAG-3′ 5′-AGTCTCATTCCAGCCAGTGC-3′

IL-6 (5′-CTCAGCCCTGAGAAAGGAGA-3′ 5′-CCAGGCAAGTCTCCTCATTG-3′)

IP-10 (5′-TGGCATTCAAGGAGGTACCTCTC-3′ 5′-TGATCTCAACACGTGGACAAA-3′)

CASP8 (5′-AGAGTCTGTGCCCAAATCAAC-3′ 5′-GCTGCTTCTCTCTTTGCTGAA-3′)

BAX (5′-TCCCCCCGAGAGGTCTTTT-3′ 5′-CGGCCCCAGTTGAAGTTG-3′)

BAK (5′-CATCAACCGACGCTATGACTC-3′ 5′-GTCAGGCCATGCTGGTAGAC-3′)

PRKCE (5′-CAACGGACGCAAGATCGAG-3′ 5′-CTGGCTCCAGATCAATCCAGT-3′)

XIAP (5′-TTTGCCTTAGACAGGCCATC-3′ 5′-TTTCCACCACAACAAAAGCA-3′)

Survivin (5′-AGAACTGGCCCTTCTTGGAGG -3′ 5′-CTTTTTATGTTCCTCTATGGGGTC-3′)

cIAP1 (5′-AGCTAGTCTGGGATCCACCTC-3′ 5′-GGGGTTAGTCCTCGATGAAG-3′)

TRAIL (5′-AGCAATGCCACTTTTGGAGT-3′ 5′-TTCACAGTGCTCCTGCAGTC-3′)

Fluorescence-activated cell sorting cytometry analysis

Cells were stained with FITC labeled Annexin V and propidium iodide (Invitrogen) based on the manufacturer's instructions. Stained cells were analyzed using a FACS Aria III (Becton Dickinson), and data were analyzed by using FlowJo software (FlowJo, Ashland, OR, USA).

RNA-seq analysis

Cells were harvested in TRIzol; total RNA was isolated and assessed for quality. cDNA libraries were prepared using TruSeq technology according to the manufacturer's protocol (Illumina, San Diego, CA). Libraries were sequenced using NextSeq500 with a read length (2 × 75 bp) by Eurofins Genomic India Private Limited, India. FastQC was used to assess the read quality of raw data Trimmomatic was used to

remove the Illumina adaptors and filter the reads using a sliding window approach (Bolger et al., 2014). Approximately 20 million cleaned pair-end sequencing reads from each sample were uploaded to the Galaxy web platform and were analyzed at https://usegalaxy.org. HISAT2 was used to map the reads with the reference human genome (hg38). Aligned RNA seq reads were assembled to transcripts, and abundance was quantified by using StringTie. Differential expression analysis of genes between groups was done using DESeq2 (Love et al., 2014). Various R packages were used to visualize the expression and differential expression outcomes. Gene ontology (GO) analysis was done using the web-based Gene Set Analysis toolkit, and analysis of upregulated KEGG pathways was done using Enrichr. Cluster 3.0 and TreeView 1.1.6 were used for making heat maps.

Enzyme-linked immunosorbent assay (ELISA)

Scrambled (shSCR) or IFI16 (shIFI16) knocked down A549 were infected with IAV or NDV, and culture supernatants were collected 36 to 40hr post-infection and analyzed for IL-6 and IP-10 cytokines according to the manufacture's protocol (Becton Dickinson).

Western blotting analysis

For endogenous detection of protein, scrambled (shSCR) or IFI16 (shIFI16) knocked down A549 cells (grown in a 6 well plate) were lysed in 30 μL of standard cell lysis buffer, and ~8 μg of protein was loaded to each well. Immunoblotting was done as using anti-β actin, anti-γ Tubulin, anti-Caspase3, anti-Caspase1, anti-flag, and anti-IFI16 antibody following stand western blotting protocol (Sathish et al., 2009).

ImageJ image analysis

For Western blot densitometry, in the immunoblots, an area of interest was selected on the smeary part above the bands, and the mean density of the selected area was calculated.

RNA immunoprecipitation

Cells infected with IAV 24 h post-transfection were harvested using standard lysis buffer supplemented with 1x protease inhibitor cocktail (Sigma Aldrich). 1/10 of the lysate was taken as input control. Immunoprecipitation was done using M2 flag affinity beads (Sigma) by incubating overnight with the lysate followed by multiple washes as per the manufacturer's instruction. The RNA was isolated from the input, and the immunoprecipitated fraction using the TRIzol reagent and cDNA was made. Further, the pull-down viral RNA expression was quantified using qPCR. Fold differences in viral RNA levels relative to RIG-I were determined using the following equation: $2-\Delta\Delta Ct = [(Ct\ sample\ pulldown - Ct\ sample\ input)] - [(Ct\ RIG-I\ pulldown - Ct\ RIG-I\ input)$ (Thapa et al., 2016).

Caspase-1 assay

Caspase 1 activity was determined using FAM-FLICA caspase1 assay kit (Immunochemistry Technologies) following the manufacturer's protocol.

QUANTIFICATION AND STATISTICAL ANALYSIS

All the experiments were done with appropriate controls, as mentioned in the legends. Experiments were carried out with triplicates or duplicates at least three times independently. GraphPad Prism 5.0 (GraphPad Software, La Jolla, CA, USA) was used for statistical analysis and plotting Graphs. Differences between the two groups were compared by an unpaired, two-tailed Student's t-test, and differences between three groups or more were compared by ANOVA with the Newman-Keuls test. Differences were considered to be statistically significant when p value $p < 0.05$. Statistical significance in the figures is indicated as follows: ***$p < 0.001$, **$p < 0.01$, *$p < 0.05$; ns, not significant.